Clinicopathological and molecular features of a series of 41 biphenotypic sinonasal sarcomas expanding their molecular spectrum

F Le Loarer, MD, PhD[1,2,3,*], **S Laffont, MD**[1,*], **T Lesluyes, MSc**[2,3,4], **F Tirode, PhD**[5,6], **C Antonescu, MD**[7], **AC Baglin, MD**[8], **L Delespaul, MSc**[2,3,4], **I Soubeyran, MD, PhD**[1,3], **I Hostein, PhD**[1], **G Pérot, PhD**[1], **F Chibon, PhD**[3,4], **J Baud, PhD**[3], **S Le Guellec, MD**[9], **M Karanian, MD**[5,6,10], **V Costes-Martineau, MD**[11], **C Castain, MD**[12], **S Eimer, MD**[12], **B Le Bail, MD**[2,12], **M Wassef, MD**[8,¶], **JM Coindre, MD**[1,2,3,¶]

[1]Department of Pathology, Institut Bergonie, Bordeaux, France.

[2]Université de Bordeaux, Talence, France.

[3]INSERM U1218 ACTION, Bordeaux, France

[4]Centre de Recherche en Cancérologie de Toulouse, Toulouse, France.

[5]Univ Lyon, Université Claude Bernard Lyon 1, INSERM 1052, CNRS 5286, Cancer Research Center of Lyon, Lyon, France

[6]Department of Translational Research and Innovation, Centre Leon Berard, Lyon, France

[7]Department of Pathology, Memorial Sloan Kettering Cancer Center, New York, USA

[8]Department of Pathology, Hôpital Lariboisiere, Paris, France

[9]Department of Pathology, Institut Claudius Regaud, Institut Universitaire du Cancer Toulouse-Oncopole, Toulouse, France.

[10]Department of Pathology, Centre Leon Berard, Lyon, France.

[11]Department of Pathology, CHU de Montpellier, Montpellier, France

[12]Department of Pathology, CHU de Bordeaux, Bordeaux, France

Abstract

Biphenotypic sinonasal sarcoma (BSNS) is a locally aggressive tumor occurring in the sinonasal region. It harbors both myogenic and neural differentiation and is characterized by *PAX3* rearrangement with *MAML3* as the most frequent fusion partner, but the partner of *PAX3* remains unidentified in a subset of cases. About 70 cases have been reported so far. In this study, we report a series of 41 cases with clinical, pathological and molecular description. Twenty-five (61%) patients were female and median age was 49 years. Tumors arose predominantly in the nasal

Correspondence Pr Jean-Michel Coindre, Phone: +33 556 33 33 29, Fax: +33 556 33 04 38, j.coindre@bordeaux.unicancer.fr.
*These authors contributed equally: François Le Loarer, Sophie Laffont
¶These authors jointly supervised the work: Michel Wassef, Jean-Michel Coindre

cavity and ethmoidal sinuses. Local recurrences occurred in 8 cases out of the 25 (32%). Histological features were characteristic of BSNS with 5 cases showing focal rhabdomyoblastic differentiation. Immunohistochemistry showed a constant positivity of S100 protein and PAX3 and negativity of SOX10. MyoD1 was focally positive in 91% of cases whereas only 20% were positive for myogenin. Molecular analysis showed a *PAX3-MAML3* transcript in 37 cases (90%). RNA sequencing was performed in the 4 negative cases for *PAX3-MAML3* fusion and showed that one case harbored a *PAX3-FOXO1* fusion as previously described in the literature and two novel fusions: *PAX3-WWTR1* fusion in 2 cases and *PAX3-NCOA2* fusion in one case. RNA sequencing results were confirmed by FISH, RT-PCR and Sanger sequencing. The *PAX3-NCOA2*-positive case showed focal rhabdomyoblastic differentiation. In conclusion, we report two novel fusions (*PAX3-WWTR1* and *PAX3-NCOA2)* in BSNS and show that MyoD1 is more sensitive than myogenin for demonstrating myogenic differentiation in this tumor.

Keywords

Biphenotypic sinonasal sarcoma; PAX3; MAML3; FOXO1; WWTR1; NCOA2

Introduction

Biphenotypic sinonasal sarcoma (BSNS), also known as low-grade sinonasal sarcoma with neural and myogenic features, is a locally aggressive tumor occurring in the sinonasal region, first delineated at the morphological level by Lewis JT et al in 2012 (1). In 2014, these tumors were shown to harbor a recurrent *PAX3-MAML3* fusion (2). In 2016, Huang SC (3) and Wong WJ et al (4) reported respectively 2 cases with a *PAX3-NCOA1* and one case with a *PAX3-FOXO1* fusion. The same year, Fritchie KJ et al (5) reassessed the Mayo Clinic series initially studied by Lewis JT et al and Wang X et al. In this larger series of 44 SNS, they reported 24 cases with a *PAX3-MAML3* fusion, 3 with a *PAX3-FOXO1* fusion and one with a *PAX3-NCOA1* fusion, whereas 11 cases showed a *PAX3* rearrangement with no defined partner, one case showed a *MAML3* rearrangement with no defined partner and 4 were negative for *PAX3, MAML3, FOXO1, NCOA1* and *NCOA2* genes.

We investigated a retrospective and prospective series of 41 cases at clinical, histological, immunohistochemical and molecular levels. Our findings expand the molecular spectrum of these lesions with the description of two previously unreported fusion variants, *PAX3-NCOA2* and *PAX3-WWTR1.*

Materials and methods

Selection of cases

Ethics approval from the appropriate committees was obtained. All sarcoma cases are recorded in the national sarcoma pathology RREPS database, approved by the National Committee for Protection of Personal Data (CNIL, n°910390), in compliance with the ethics principles of the Helsinki Declaration.

Formalin-fixed paraffin-embedded specimens diagnosed between January 2000 and June 2018 were retrieved from the archives of the pathology departments involved in the French

soft tissue (RRePS) and head and neck (REFCOR) pathology networks. Forty-four cases were identified but three cases were excluded as the available material was not suitable for molecular analysis. The following clinical data were collected: gender, age at diagnosis, location and size of tumor, initial treatment and follow-up. All cases were microscopically reviewed by two pathologists (SL, JMC).

Immunohistochemistry

The tissue slides were deparaffinized in xylene, hydrated in alcohol, and baked in a microwave (30 min in Trisbuffer, pH 9). Endogenous peroxidase was blocked. Staining was performed on the Benchmark ultra-automated stainer (Ventana) using diamino-benzidine as chromogen (Dako, Glostrup, Denmark). The following antibodies were used: Pankeratin AE1/AE3 (clone PCK26, pre-diluted; Ventana Media Systems, Tucson, AZ ,USA); EMA (clone E29, pre-diluted; Ventana Media Systems, Tucson, Arizona ,USA); S100 protein (clone poly Z311, dilution 1:500; Dako, Glostrup, Denmark); smooth muscle actin (clone 1A4, dilution 1:12000; Sigma Aldrich, Saint Louis, MO, USA); desmin (clone DE-R-11, pre-diluted; Ventana Media Systems, Tucson, Arizona USA); myogenin (clone LO 26, dilution 1:20; Leica Biosystems, Buffalo Grove, IL, USA); MyoD1 (clone EP212, pre-diluted; Cell Marque, Rocklin, CA, USA); CD34 (clone QBEnd10, pre-diluted; Ventana, Tucson, AZ, USA); beta-catenin (clone 14, pre-diluted; Cell Marque, Rocklin, CA, USA); SOX10 (clone EP268, dilution 1:100; BioSB, Santa Barbara, CA, USA); H3K27Me3 (clone C36B11, dilution 1:200; Cell Signaling Technology, Danvers, MA, USA); PAX3 (clone 274212, dilution 1:100; RD Systems Europe, Lille, France)

For myogenin, MyoD1, SOX10, H3K27me3 beta-catenin and PAX3, only a nuclear staining was considered as positive.

Fluorescence *In situ* Hybridization

FISH analyses on interphase nuclei from paraffin-embedded 4-μm-thick sections were performed by applying custom probes using bacterial artificial chromosomes (BACs), flanking *PAX3, MAML3, NCOA1* genes according to the procedure previously described (3).

FISH analysis for *FOXO1, NCOA2* and *WWTR1* was performed with 4-μm sections of formalin-fixed paraffin-embedded tissue and the Histology FISH Accessory Kit (Agilent K5799, Dako, Glostrup, Denmark) using commercially available break apart probes covering *FOXO1* (Zytovision, Zytolight spec Z-2208–200), *NCOA2* (Empire genomics, EG-NCOA2BA-20-ORGR) and *WWTR1*(Zytovision, Zytolight spec Z-2212–50).

RNA extraction for Real-Time RT-PCR and Paired-end RNA-sequencing

Total RNA was extracted from formalin-fixed paraffin-embedded tissue section using Trizol reagent (Thermo Fisher Scientific, Courtaboeuf, France) according to the manufacturers' recommendations. DNA was removed using RNase-free DNase set (Qiagen) followed by a second Trizol extraction. The yield of total RNA obtained was evaluated using NanoDrop (Thermo Fisher Scientific).

Reverse Transcription-Polymerase Chain Reaction analysis for *PAX3-MAML3, PAX3-FOXO1, PAX3-NCOA2* and *PAX3-WWTR1* fusion genes

Real-time RT-PCR, using Taqman technology according to the technique previously described by Hostein et al (6), was performed for *PAX3-MAML3* and *PAX3-FOXO1* fusion genes.

For *PAX3-MAML3* gene fusion, the following primers and probe were used:

PAX3 forward primer: 5'-TTT CCA GCT ATA CAG ACA GCT TTG-3'

MAML3 reverse primer: 5'-TCC TTC CAA CTT CCT TTT CAC AGT-3'

Probe: 5'-FAM-AACCCCACCATTGGCAATGGCCT-TAMRA-3'

For *PAX3-FOXO1* gene fusion, the following primers and probe were used:

PAX3 forward primer: 5'-TTG GCA ATG GCC TCT CAC C-3'

FOXO1 reverse primer: 5'-ATC CAC CAA GAA CTT TTT CCA G-3'

Probe: 5'-TET-CCCTAC ACA GCA AGT TCA TTC GTG TGC AG-TAMRA-3'

Conventional RT-PCR was performed for *PAX3-NCOA2* and *PAX3-WWTR1* fusion genes.

An aliquot of the RNA extracted from FFPE tissue was used to confirm the novel fusion transcripts identified. One microgram of total RNA was reverse-transcribed in cDNA with the High Capacity cDNA Reverse Transcription Kit with RNase Inhibitor (Invitrogen, cat. No. 4374966). PCR was performed using the AmpliTaq Gold™ DNA Polymerase kit (Applied Biosystems™, cat. No. 4311806) on 50 ng of cDNA with the following primers: PAX3_FWD: 5' GACCCTGTCACAGGCTAC 3' and WWTR1_REV: 5' TCTGCTGGCTCAGGGTACT 3' and for the reciprocal transcript: WWTR1_FWD: 5' CACACCAGTGCCTCAGAG 3' and PAX3_REV: 5' CGTGTTCAAAAGGATTTGAAACC 3'. For PAX3-NCOA2 validation, the following primers were used: PAX3_FWD: 5' CTTTGTGCCTCCGTCGGG 3' and NCOA2_REV: 5' CTCGTGTCTGGGAAAAGCTG 3'. The Touchdown 60°C program was used (TD 60°C; two cycles at 60°C, followed by two cycles at 59°C, two cycles at 58°C, three cycles at 57°C, three cycles at 56°C, four cycles at 55°C, four cycles at 54°C, five cycles at 53°C, and finally 10 cycles at 52°C). PCR products were then purified using the Illustra ExoProStar™ PCR Purification Kit (GE Healthcare, cat. No. US77702), and sequencing reactions were performed with the Big Dye Terminator V1.1 Kit (Applied Biosystems, cat. No. 4337450). After purification with the Big Dye XTerminator Purification Kit (Applied Biosystems,cat. No. 4376486), the samples were sequenced on a 3130xl Genetic Analyzer (Applied Biosystems).

Paired-end RNA sequencing

Four cases were studied by RNA sequencing with formalin-fixed paraffin-embedded material (cases 5, 8, 29 and 40). All samples had a percentage of RNA fragments above 200

nucleotides (DV200) above 13% upon Tape Station analysis using the Hs RNA Screen Tape (Agilent).

Libraries were prepared with 100 ng of total RNA using the TruSeq RNA Access Library Prep Kit (Illumina, San Diego, USA). Libraries were pooled by groups of 12 samples. Paired-end sequencing was performed using the NextSeq 500/550 High Output V2 kit (150 cycles) on an Illumina NextSeq 500 platform (Illumina, San Diego, CA).

Sequencing data (average of 65 million reads per sample) were aligned with STAR on GRCh 38 reference genome. The fusion transcripts were called with STAR-Fusion, FusionMap, FusionCatcher, ERICSCRIPT and TopHat-fusion and validated if present in the fusion list of at least two algorithms (7–11).

Results

Clinical features

A total of 41 cases were included in this study. Patient characteristics and clinical follow-up are presented in Table 1. Sixteen patients were male (39%) and 25 female (61%). The mean and median ages at diagnosis were 52.2 and 49 years, respectively (range 25–84). Tumors arose predominantly in the nasal cavity (28 cases, 68%), ethmoid sinuses (20 cases, 49%) with 11 cases in both the nasal cavity and ethmoid sinuses (27%). Seven cases (17%) arose in the facial sinuses NOS and 6 cases (15%) showed an extensive tumor with involvement of the sinuses and adjacent bones. Tumor size was known in 17 cases and ranged from 10 to 90 mm (median size 35 mm).

Treatment was known in 33 patients and consisted in surgery for 32, with radiotherapy in 9 patients, chemotherapy in 2 and radiotherapy and chemotherapy in 2 patients.

Clinical follow-up varied from 11 to 185 months (median 45 months) and was available for 25 patients of the cohort with 8 recent cases. Local recurrences occurred in 8 cases (32%) at 9 to 95 months of follow-up. No patient showed evidence of distant metastasis.

Pathological features (Figures 1 and 2)

Initial diagnosis was schwannoma (n=6), neurofibroma (n=1), MPNST (n=13, with rhabdomyoblastic differentiation in 5 cases), synovial sarcoma (n=1), fibrosarcoma (n=3) and low-grade sinonasal sarcoma (n=17). Out of 20 cases seen after 2014, 17 were properly classified by the initial pathologist. Final diagnosis of BSNS was based on histology and immunohistochemistry according to the original description (1). The histologic characteristics are highly reproducible and diagnosis is easy in most cases.

Tumors were poorly circumscribed with infiltrative involvement of surrounding tissues, particularly sinonasal bones (19 out of 33 samples containing bone tissues). Twenty-five cases showed hyperplasia of the overlying respiratory epithelium with entrapment of benign glands in the tumor. The tumors consisted of hypercellular proliferation of monotonous spindle cells arranged in fascicles, often with a herringbone pattern. The cellularity was typically high with usually scanty collagen and focally myxoid changes in 7 cases. A

hemangiopericytoma-like pattern was focally present in 33 cases. Tumor cells were uniform with a monotonous elongated hyperchromatic nucleus with fine granular chromatin and a small amount of cytoplasm with indistinct borders. Pleomorphic cells were visible focally in only one case (Figure 2). Cells with abundant eosinophilic cytoplasm in favor of rhabdomyoblastic differentiation were present in 5 cases (cases 5, 6, 7, 14 and 16). Mitotic activity was low in most cases (from 0 to 4 mitoses per 10 high power fields, median count 1), but 2 cases showed 9 and 12 mitoses per 10 high-power fields. Necrosis was always absent.

Immunohistochemical features (Figure 3)

Results are summarized in Table 2. All 41 cases (100%) showed focal (56%) or diffuse (44%) positivity for S100 protein whereas SOX10 was negative in all cases tested. H3K27me3 was retained in 33% of cases and partial loss in 67% of cases (median, 65% of positive tumor cells). Smooth muscle actin was positive in 90% of cases, desmin in 66%, myogenin in 20% and MyoD1 in 91%. Desmin, myogenin and MyoD1 were positive only focally. PAX3 was positive in 29 cases tested with 21 cases showing a diffuse positivity (strong positivity in 14 and weak in 7 cases) and 8 cases with a focal positivity (strong positivity in 2 cases and weak in 6 cases). Nuclear beta-catenin was focally positive in 26% of cases. Pankeratin AE1/AE3, EMA and CD34 were focally positive in 11, 11 and 10% of cases, respectively.

Molecular biological features

Initially, 44 cases were screened with RT-PCR for *PAX3-MAML3*: 35 cases were positive, 5 negative and 4 non-interpretable because of nucleic acid degradation. Then, 8 of these negative or non-interpretable cases were screened with FISH for probes for *PAX3*: 5 were positive and 3 non-interpretable. These 3 non-interpretable cases for RT-PCR and FISH were excluded from the study because of nucleic acid degradation. Among the 5 positive cases with FISH for *PAX3*, 2 were positive with FISH for *MAML3* (cases 9 and 15) and 3 were negative. These 3 negative cases (cases 5, 8 and 29) were also negative with FISH for *NCOA1* and *FOXO1*. These 3 cases as well as case 40 (recent case negative for initial RT-PCR) were analyzed by RNA sequencing. This revealed a fusion transcript which was confirmed by both RT-PCR and FISH: *PAX3-NCOA2* (case 5), *PAX3-WWTR1* (cases 8 and 29) and *PAX3-FOXO1* (case 40). Fusion transcripts *PAX3-NCOA2* and *PAX3-WWTR1* were also confirmed by Sanger sequencing (Figures 4 and 5). They were both in frame fusions involving *PAX3* exon 7 with *NCOA2* exon 12 and *PAX3* exon 8 with *WWTR1* exon 5, respectively.

Discussion

To our knowledge, three series of biphenotypic sinonasal sarcoma have been published with 44, 11 and 15 cases, respectively (5, 12, 13). We report here the second largest series with 41 cases. We confirm that this tumor is locally aggressive with frequent bone destruction and local recurrence but with no distant metastasis. It occurs in the nasal cavity and/or paranasal sinuses, predominantly in middle-aged females. Histologically, BSNS is a poorly circumscribed and hypercellular proliferation of monotonous spindle cells with a low mitotic

rate and, frequently, entrapped hyperplastic surface epithelium. In our series, only one case showed focal pleomorphic cells, 2 cases showed some mitotic activity and focal myxoid changes were present in 7 cases. We also confirm previously published data, with consistent at least focal S100 protein positivity, frequent positivity with muscle markers, and negativity for SOX10, epithelial markers and CD34. As recently reported by Jo VY et al (13), all our tested tumors were PAX3-positive but with weak and/or focal positivity in about half of them. Regarding muscle markers, we found frequent focal positivity for MyoD1 (91% of cases) but a much lower rate of positivity for myogenin (20%). This is in agreement with the expression profiling reported by Wang X et al (2) in 8 cases of BSNS. In that study, MyoD1 was one of the top 150 overexpressed genes. However, they observed a focal expression of MyoD1 in only 4 out of 25 cases whereas we found positivity in 91% of our cases. This difference may be due to the different antibodies used in the studies (clone 5.8 A by Wang X et al and clone EP212 in our study). Unlike Rooper LM et al (12) who reported an almost constant nuclear positivity for beta-catenin, only 26% of our cases showed focal nuclear positivity. Therefore, other studies are necessary to evaluate the usefulness of this marker in BSNS.

A recurrent *PAX3-MAML3* fusion event is present in most BSNS with a few cases showing alternative fusion of *PAX3* with *NCOA1* and *FOXO1*. In their series of 44 cases, Fritchie KJ et al (5) reported 24 cases with a *PAX3-MAML3*, 3 cases with a *PAX3-FOXO1* and 1 case with a *PAX3-NCOA1* fusion gene, whereas 11 cases showed a *PAX3* rearrangement but with no rearrangement of *MAML3, FOXO1, NCOA1* and *NCOA2* genes. In the present study, 37 cases showed a *PAX3-MAML3* fusion, 2 cases a *PAX3-WWTR1* fusion, 1 case a *PAX3-FOXO1* fusion and 1 case a *PAX3-NCOA2* fusion. Given the structural and functional similarity of the MAML3, FOXO1, NCOA1 and NCOA2 proteins, the presence of a *PAX3-NCOA2* fusion transcript in BSNS was expected (5). Like the 2 cases of BSNS with a *NCOA1* rearrangement reported by Huang SC et al (3), our case with a *NCOA2* rearrangement showed focal rhabdomyoblastic differentiation. *PAX3-WWTR1* is a new fusion in BSNS. WWTR1, also known as TAZ, is a transcriptional co-activator with a PDZ binding motif. In mammals, *YAP1* and *WWTR1* are downstream effectors of the Hippo signaling pathway, which is an evolutionarily conserved network that plays a central role in regulating cell proliferation and cell fate to control organ growth and regeneration. The Hippo pathway controls gene expression by inhibiting the activity of *YAP1* and *WWTR1*. Hyperactivity of these two genes promotes uncontrolled cell proliferation, impairs differentiation, and is associated with cancer (14). A *WWTR1-CAMTA1* fusion has been shown in epithelioid hemangioendothelioma and is now a key diagnostic tool for this rare tumor (15). BSNS is a second example of the direct role of *WWTR1* in the development of a cancer. Recently, Sun C et al (16) reported the important role of *YAP1* and *WWTR1* in skeletal muscle stem cell function. They showed that *YAP1* and *WWTR1* play a similar role in promoting myoblastic proliferation, and that during the later stage of myogenesis, *WWTR1* switches toward influencing satellite cell fate by promoting myogenic differentiation. *YAP1* and *WWTR1* have many common target genes, but *WWTR1* regulates some genes independently of *YAP1*, including myogenic genes such as *PAX7, MYF5* and *MYOD1*.

In conclusion, this is the second largest series of BSNS. We report two new fusion transcripts, *PAX3-NCOA2* and *PAX3-WWTR1,* and confirm the major value of immunohistochemistry for the diagnosis with constant positivity of S100 protein and PAX3 associated with negativity of SOX10. Moreover, we found that MyoD1 is more sensitive than myogenin for demonstrating myogenic differentiation in this tumor.

Acknowledgments

References

1. Lewis JT, Oliveira AM, Nascimento AG, Schembri-Wismayer D, Moore EA, Olsen KD, et al. Low-grade sinonasal sarcoma with neural and myogenic features: a clinicopathologic analysis of 28 cases. Am J Surg Pathol 2012;36:517–25. [PubMed: 22301502]

2. Wang X, Bledsoe KL, Graham RP, Asmann YW, Viswanatha DS, Lewis JE, et al. Recurrent PAX3-MAML3 fusion in biphenotypic sinonasal sarcoma. Nat Genet 2014;46:666–8. [PubMed: 24859338]

3. Huang S-C, Ghossein RA, Bishop JA, Zhang L, Chen T-C, Huang H-Y, et al. Novel PAX3-NCOA1 fusions in biphenotypic sinonasal sarcoma with focal rhabdomyoblastic differentiation. Am J Surg Pathol 2016;40:51–9. [PubMed: 26371783]

4. Wong WJ, Lauria A, Hornick JL, Xiao S, Fletcher JA, Marino-Enriquez A. Alternate PAX3-FOXO1 oncogenic fusion in biphenotypic sinonasal sarcoma. Genes Chromosomes Cancer 2016;55:25–9. [PubMed: 26355893]

5. Fritchie KJ, Jin L, Wang X, Graham RP, Torbenson MS, Lewis JE, et al. Fusion gene profile of biphenotypic sinonasal sarcoma: an analysis of 44 cases. Histopathology 2016;69:930–6. [PubMed: 27454570]

6. Hostein I, Andraud-Fregeville M, Guillou L et al. Rhabdomyosarcoma: value of myogenin expression analysis and molecular testing in diagnosing the alveolar subtype. An analysis of 109 paraffin-embedded specimen. Cancer 2004;101:2817–24. [PubMed: 15536621]

7. Ge H, Liu K, Juan T et al. FusionMap: detecting fusion genes from next-generation sequencing data at base-pair resolution. Bioinformatics 2011;27:1922–8. [PubMed: 21593131]

8. Trapnell C, Roberts A, Goff L, et al. Differential gene and transcript expression analysis of RNA-seq experiments with TopHat and Cufflinks. Nature protocols 2012;7:562–578. [PubMed: 22383036]

9. Lagstad S, Zhao S, Hoff AM, et al. chimeraviz: a tool for visualizing chimeric RNA. Bioinformatics 2017;33:2954–6.3. [PubMed: 28525538]

10. Nicorici DSM, Edgren H, Kangaspeska S, Murumagi A, Kallioniemi O, Virtanen S, Kilkku O FusionCatcher - a tool for finding somatic fusion genes in paired-end RNA-sequencing data. bioRxiv 2014.

11. Benelli M, Pescucci C, Marseglia G, et al. Discovering chimeric transcripts in paired-end RNA-seq data by using EricScript. Bioinformatics 2012;28:3232–3239. [PubMed: 23093608]

12. Rooper LM, Huang S-C, Antonescu CR, Westra WH, Bishop JA. Biphenotypic sinonasal sarcoma: an expanded immunoprofile including consistent nuclear β-catenin positivity and absence of SOX10 expression. Hum Pathol 2016;55:44–50. [PubMed: 27137987]

13. Jo VY, Mariño-Enriquez A, Fletcher CDM, Hornick JL. Expression of PAX3 distinguishes biphenotypic sinonasal sarcoma from histologic mimics. Am J Surg Pathol 2018;42:1275–85. [PubMed: 29863547]

14. Misra JR, Irvine KD. The Hippo signaling network and its biological functions. Annu Rev Genet 2018;52:3.1–3.23.

15. Errani C, Zhang L, Sung YS et al. A novel WWTR1-CAMTA1 gene fusion is a consistent abnormality in epithelioid hemangioendothelioma of different anatomic sites. Gens Chromosomes Cancer 2011;50:644–53.

16. Sun C, De Mello V, Mohamed A et al. Common and distinctive functions of the Hippo effectors Taz and Yap in skeletal muscle stem cell function. Stem Cells 2017;35:1958–72. [PubMed: 28589555]
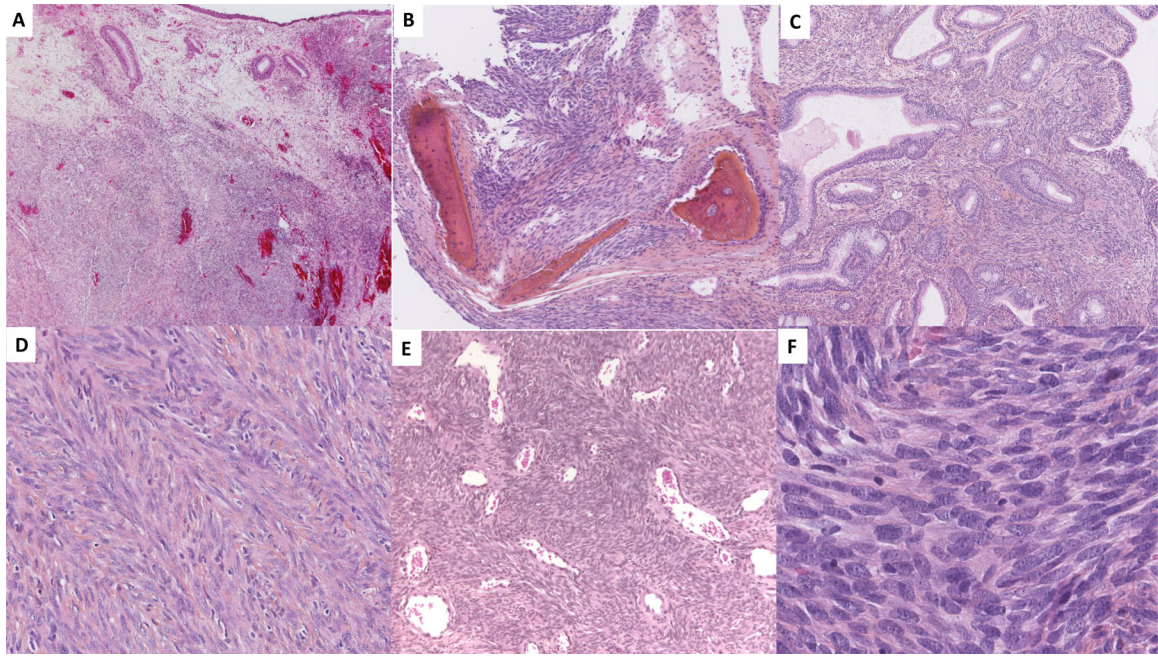
Figure 1:
Main histological features of biphenotypic sinonasal sarcoma. Tumor is poorly circumscribed (A) with frequent involvement of sinonasal bones (B). Hyperplasia of overlying respiratory epithelium with entrapment of benign glands by tumor cells is a typical feature (C). Tumor is composed of hypercellular proliferation of monomorphic spindle cells arranged in medium-to-long fascicles, often with a herringbone pattern (D). Hemangiopericytoma-like pattern is common (E). Tumor cells are uniform with monotonous spindle nucleus and low mitotic activity (F).
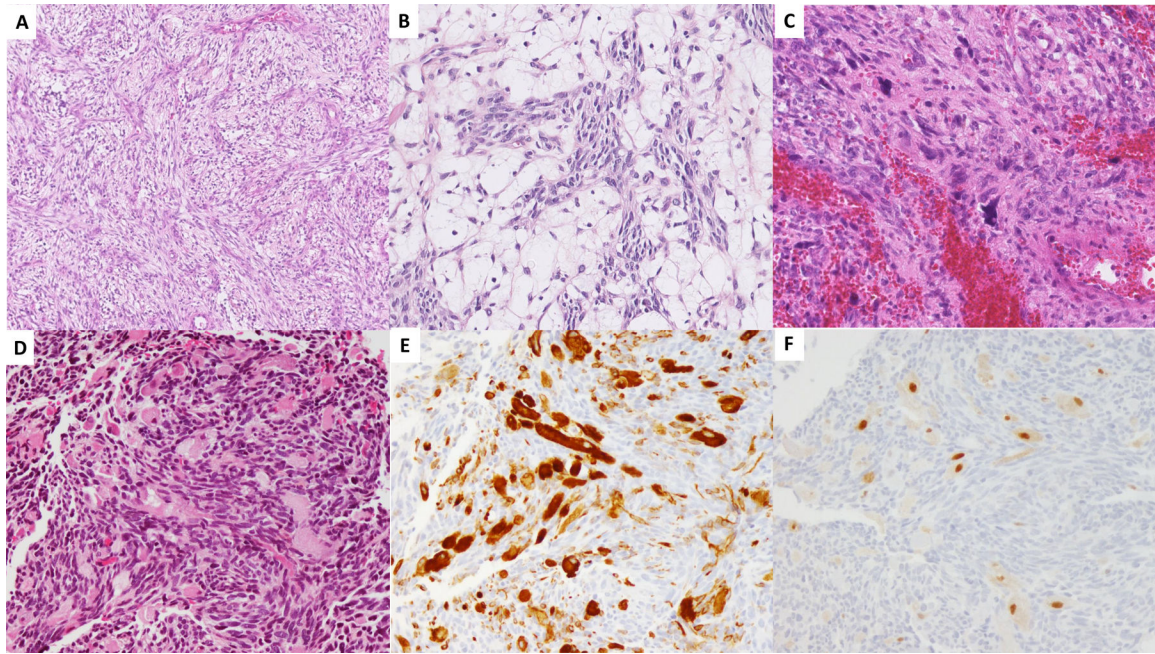
Figure 2:
Rare morphologic patterns of biphenotypic sinonasal sarcoma. Myxoid changes may be focally present (A). Focal chronic inflammatory infiltrate is rare. One case (#5) showed a histiocytic infiltrate (B). Only one case (#19) showed focal nuclear atypia (C). Focal rhabdomyoblastic differentiation was present in 5 cases with large round or elongated cells with abundant eosinophilic cytoplasm (D) and focal cross-striation. Desmin (E) and myogenin were always positive in these areas.
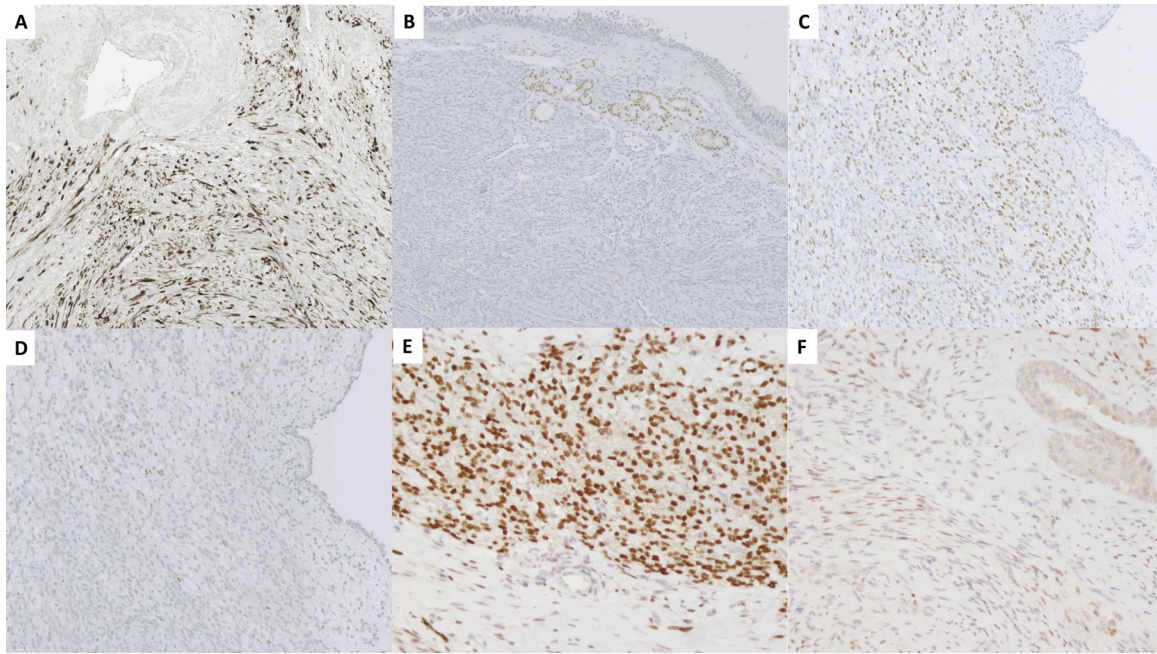
Figure 3:

Immunohistochemical profile of biphenotypic sinonasal sarcoma. S100 protein was always positive focally or diffusely (A) whereas SOX 10 was always negative (B). MyoD1 was positive in about 90% of cases (C). Myogenin was focally positive in only 20% of cases (D). PAX3 was positive in all tested cases, strongly and diffusely in about half of them (E) but weakly and/or focally in the other cases with a background in some cases (F).
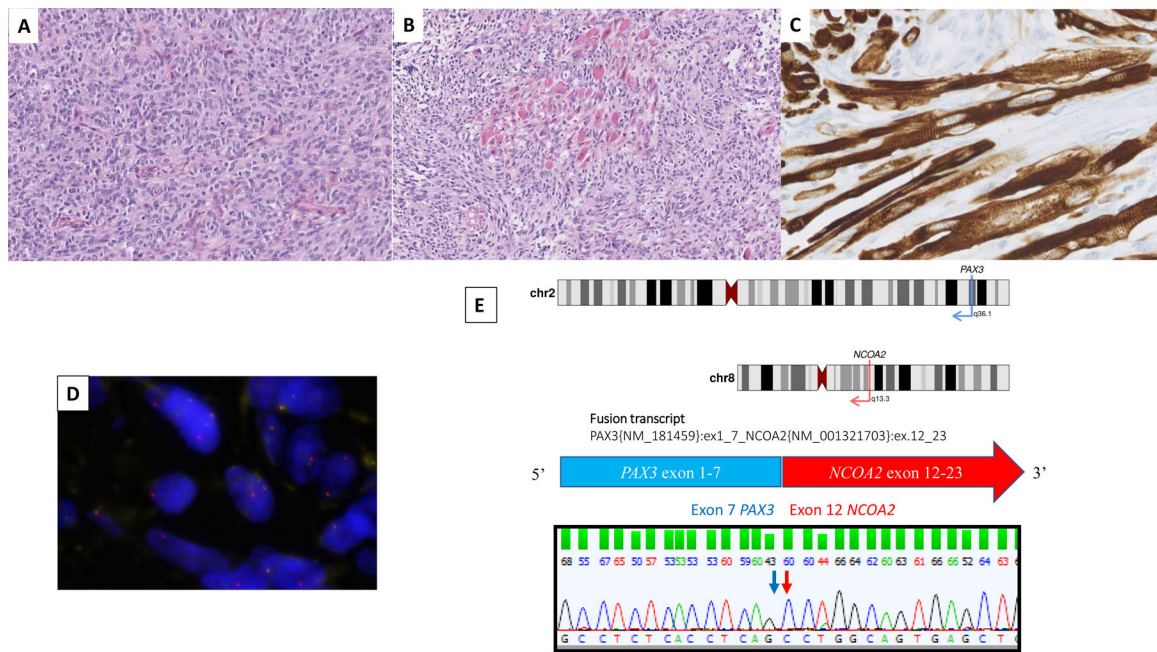
Figure 4:

Novel *PAX3-NCOA2* fusion in biphenotypic sinonasal sarcoma (Case 5). Typical aspect of BSNS (A) with areas showing rhabdomyoblastic differentiation (B). Immunohistochemistry with desmin highlights cross-striations (C). Fluorescence *in situ* hybridization (FISH) using a break-apart probe shows a rearrangement of *NCOA2* (D). E. Structure of *PAX3-NCOA2* fusion transcript. From up to bottom: schematic representing locus and chromosomal positions of *PAX3* and *NCOA2*; schematic of breakpoint positions involving *PAX3* exon 7 and *NCOA2* exon 12; nucleotidic sequence of adjoined sequences.
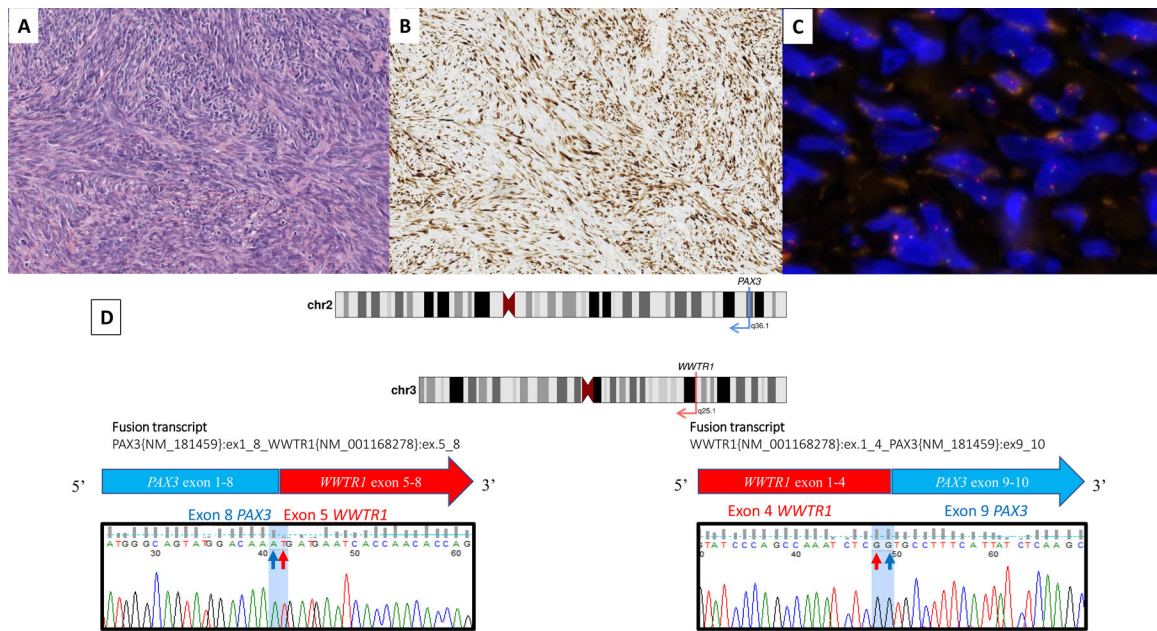
Figure 5:

Novel *PAX3-WWTR1* fusion in biphenotypic sinonasal sarcoma (Cases 8 and 29). Typical aspect of BSNS (A-case 8) with diffuse positivity of S100 protein (B-case 8). Fluorescence *in situ* hybridization (FISH) using a break-apart probe shows a rearrangement of *WWTR1* (C-case 29). D. From up to bottom: schematic representing locus and chromosomal positions of *PAX3* and *WWTR1*; schematic of breakpoint positions involving *PAX3* exon 8 and *WWTR1* exon 5 for both cases, and associated reciprocal fusion transcript *WWTR1* exon 4 and *PAX3* exon 10 for cases 29; nucleotidic sequence of adjoined sequences for cases 8 and 29.

Table 1 :

Clinical and follow-up data in a series of 41 biphenotypic sinonasal sarcomas.

Case	Sex	Age	Site of tumor	Treatment modalities	Local Recurrence (months)	Follow-up (months)	Status
1	F	69	Sinus (ethmoid)	Surgery	Yes (36m)	185	AWD
2	F	25	Nasal cavity	Surgery	No	175	NED
3	M	35	Nasal cavity	NA	NA	NA	NA
4	F	49	Sinus (ethmoid)	Surgery	No	145	NED
5	F	49	Nasal cavity/sinus (ethmoid)	Chemotherapy, surgery, radiotherapy	No	83	NED
6	F	40	Nasal cavity/sinus (ethmoid)/cribriform plate/skull base	Surgery	NA	NA	NA
7	F	38	Sinus (NOS)	NA	NA	NA	NA
8	M	76	Nasal cavity	Surgery	No	119	NED
9	F	63	Sinus (ethmoid)/skull base/orbit	Chemotherapy, radiotherapy	Yes (91m)	102	AWD
10	F	37	Nasal cavity	Surgery, chemotherapy	No	107	NED
11	M	63	Nasal cavity	Radiotherapy, surgery	Yes (95m)	96	NED
12	F	43	Sinus (ethmoid)/skull base	Surgery, radiotherapy, chemotherapy	No	69	NED
13	M	28	Nasal cavity	Surgery	Yes (24m)	33	NED
14	F	62	Nasal cavity/sinus (ethmoid)	Surgery, chemotherapy	No	55	NED
15	F	81	Nasal cavity/sinus (ethmoid)	Surgery	NA	NA	NA
16	F	25	Nasal cavity	NA	NA	NA	NA
17	M	28	Nasal cavity	Surgery	Yes (27m)	34	NED
18	M	38	Nasal cavity	Surgery	No	54	NED
19	M	50	Nasal cavity/sinus (ethmoid/frontal)	Surgery	Yes (15m)	49	NED
20	F	84	Sinus (ethmoid/frontal)/orbit	Surgery	No	45	NED
21	M	77	Nasal cavity/sinus (ethmoid/frontal)	NA	NA	NA	NA
22	F	71	Sinus (etmoid/frontal)	Surgery	No	23	NED
23	F	77	Nasal cavity/sinus (ethmoid)/orbit/skull base	Surgery	No	17	NED
24	M	32	Nasal cavity/sinus (ethmoid/frontal)	Surgery	No	27	NED
25	M	59	Sinus (ethmoid/frontal)/orbit	Surgery, radiotherapy	No	12	NED
26	M	65	Nasal cavity/sinus (ethmoid)	Surgery, radiotherapy	Yes (11m)	23	NED
27	F	50	Nasal cavity	Surgery, radiotherapy	No	25	NED

Case	Sex	Age	Site of tumor	Treatment modalities	Local Recurrence (months)	Follow-up (months)	Status
28	F	70	Nasal cavity	Surgery	No	25	NED
29	F	65	Nasal cavity	Surgery	NA	NA	NA
30	F	49	Sinus (NOS)	NA	NA	NA	NA
31	M	29	Sinus (ethmoid)	Surgery, radiotherapy	No	20	NED
32	M	41	Nasal cavity/sinus (ethmoid)	Surgery, radiotherapy	No	18	NED
33	F	64	Nasal cavity/sinus (NOS)	Surgery	Yes (9m)	11	AWD
34	F	77	Nasal cavity/sinus (ethmoid)	Surgery	NA	Recent case	NA
35	M	38	Sinus (ethmoid)	Surgery, radiotherapy	NA	Recent case	NA
36	F	41	Sinus (NOS)	NA	NA	Recent case	NA
37	F	60	Nasal cavity/sinus (NOS)	NA	NA	Recent case	NA
38	M	65	Nasal cavity/sinus (NOS)	Surgery	NA	Recent case	NA
39	F	31	Nasal cavity	Surgery	NA	Recent case	NA
40	M	39	Nasal cavity	Surgery, radiotherapy	NA	Recent case	NA
41	F	48	Sinus (NOS)	NA	NA	Recent case	NA

Abbreviations: NA: not available; NED: no evolutive disease; AWD: alive with disease

Table 2 :

Immunohistochemical results in a series of 41 biphenotypic sinonasal sarcomas.

Antibody	Negativity (n)	Focal positivity (n)	Diffuse positivity (n)	Total positivity (%)
S100 protein	0	23	18	100
SOX10	34	0	0	0
H3K27me3	0	10	20	100
Desmin	14	27	0	66
MyoD1	3	32	0	91
Myogenin	33	8	0	20
Smooth Muscle Actin	4	28	7	90
PAX3	0	8	21	100
Beta catenin	16	5	1	27
AE1/AE3	34	4	0	11
EMA	32	4	0	11
CD34	36	4	0	10

Abbreviations: n: number of cases.